International Journal of Pharmaceutics 515 (2016) 692–701

Contents lists available at ScienceDirect

International Journal of Pharmaceutics

journal homepage: www.elsevier.com/locate/ijpharm

Radiolabeled block copolymer micelles for image-guided drug delivery

Elisabete Ribeiro[a], Irina Alho[b], Fernanda Marques[a], Lurdes Gano[a], Isabel Correia[c], João D.G. Correia[a], Sandra Casimiro[b], Luís Costa[b], Isabel Santos[a], Célia Fernandes[a,*]

[a] Centro de Ciências e Tecnologias Nucleares (C2TN), Instituto Superior Técnico, Universidade de Lisboa, Estrada Nacional 10 (km 139,7), 2695-066 Bobadela LRS, Portugal
[b] Instituto de Medicina Molecular, Faculdade de Medicina, Universidade de Lisboa, Av. Prof. Egas Moniz, 1649-028 Lisboa, Portugal
[c] Centro de Química Estrutural, Instituto Superior Técnico, Universidade de Lisboa, Av. Rovisco Pais, 1049-001 Lisboa, Portugal

ARTICLE INFO

Article history:
Received 12 July 2016
Received in revised form 7 October 2016
Accepted 2 November 2016
Available online 4 November 2016

Keywords:
PEG-*b*-PCL
Block copolymer micelle
Drug delivery system
Radiolabeled micelles
^{99m}Tc

ABSTRACT

We aimed at exploring block copolymer micelles (BCMs) for the simultaneous delivery of radiation/chemotherapy to cancer cells. To achieve that goal, we have prepared and characterized a novel type of docetaxel (DTX) loaded and non-loaded BCMs. The micelles were decorated with pyrazolyl-diamine chelating units to stabilize the matched pair ^{99m}Tc/Re for image-guided delivery of therapeutic drugs. The *in vitro* studies have shown that DTX release is pH-dependent increasing at lower pH values. Anti-proliferative studies in different cancer cell lines showed that DTX-loaded BCMs present relevant anti-proliferative activity. In comparison to free DTX, the loaded-micelles exhibited higher anti-proliferative activity for the same DTX concentration, which mean that a similar therapeutic outcome may be achieved with reduced side effects. The pyrazolyl-diamine-functionalized micelles were labeled with *fac*-$[^{99m}Tc(CO)_3(H_2O)_3]^+$ in high radiochemical yield and purity. The radiolabeled micelles are stable in phosphate buffer and in cell culture media. Cellular uptake studies in different cancer cell lines indicate a cell type and time-dependent uptake, in agreement with the anti-proliferative activity. Early biodistribution studies in healthy BALB/c mice has shown prolonged circulation lifetime in the bloodstream and relevant *in vivo* stability, important features when considering an effective DTX delivery system and image-guided delivery agent for cancer theranostics.

1. Introduction

Cancer remains one of the leading causes of death worldwide. Traditional anticancer treatments such as chemotherapy and radiotherapy are often hindered by toxicity and lack of specificity. The bioavailability and efficacy of most anticancer drugs are affected by their poor water solubility, short blood half-life, narrow therapeutic indices and high systemic toxicity (Esmaeili et al., 2009; Gothwal et al., 2016). Docetaxel (DTX) is a potent chemotherapeutic agent that is commonly administered for treatment of solid tumors, such as breast and prostate carcinomas (Esmaeili et al., 2009; Liu et al., 2011; Lu and Park, 2013). However, the clinical efficacy of DTX is limited by its fast elimination *in vivo* and poor water solubility. To overcome this disadvantage, the clinical formulation of DTX contains a high concentration of the non-ionic surfactant polysorbate 80 (Tween 80), which has been associated to hypersensitivity reactions. Moreover, side effects of DTX may require dose reduction, diminishing the treatment efficacy (Esmaeili et al., 2009; Liu et al., 2011; Palma et al., 2014).

To surpass these problems and to improve the balance between efficacy and toxicity of systemically administered anticancer agents, several drug delivery systems have been designed and evaluated to effectively transport significant amounts of these drugs to the tumor, reducing the accumulation in healthy tissues (Estanqueiro et al., 2015; Palma et al., 2014; Perez-Herrero and Fernandez-Medarde, 2015; Wicki et al., 2015).

Some nanoparticles, (Palma et al., 2014; Perez-Herrero and Fernandez-Medarde, 2015; Wicki et al., 2015) such as micelles, are considered promising drug delivery systems. In fact, micelles are nano-self-assemblies of amphiphilic copolymers which have a hydrophobic core surrounded by a hydrophilic corona. In their core several hydrophobic anticancer agents, such as DTX, can be

Abbreviations: DTX, docetaxel; BCMs, block copolymer micelles; PEG, poly (ethylene glycol); PCL, poly(ε-caprolactone); PB, phosphate buffer; DLS, dynamic light scattering; TEM, transmission electron microscopy; CMC, critical micelle concentration; LC, DTX loading content; LE, DTX loading efficiency.

* Corresponding author at: Centro de Ciências e Tecnologias Nucleares (C2TN), IST, UL, Estrada Nacional 10 (ao km 139,7), 2695-066 Bobadela LRS, Portugal.
E-mail address: celiaf@ctn.tecnico.ulisboa.pt (C. Fernandes).

http://dx.doi.org/10.1016/j.ijpharm.2016.11.004
0378-5173/

encapsulated to overcome their low aqueous solubility and to allow their transport through the blood stream to the tumor (Allen et al., 1999). Moreover, the corona can also be modified with vectors and/or imaging agents to confer specificity and/or to be used as platforms for image-guided macromolecular nanomedicine, respectively. The nature of the copolymers used to prepare micelles affects their size, surface charge, core-drug compatibility, drug loading capacity, drug release kinetics and stability. All these parameters can modulate significantly the pharmacokinetic profile and tissue distribution of the encapsulated drug (Alexis et al., 2008; Hoang et al., 2009). Indeed, it has been referred that nanodrugs with size in the range 5.5–200 nm have a long circulation time, which increases the drug accumulation in tumors by the enhanced permeability and retention (EPR) effect, one of the most important strategies to ameliorate the delivery of low-molecular weight chemotherapeutic agents to tumors (Alexis et al., 2008; Ernsting et al., 2013; Gothwal et al., 2016; Lee et al., 2010; Mikhail and Allen 2009). It has also been considered that the conjugation of poly(ethylene glycol) (PEG) to the surface of BCMs smaller than 100 nm (Ernsting et al., 2013; Mikhail and Allen 2009) reduces serum protein binding, avoids opsonisation and subsequent clearance by the mononuclear phagocytic system (MPS) (Mikhail and Allen, 2009).

Within this context, we are exploring block copolymer micelles for the simultaneous delivery of cytotoxic drugs and radiation for imaging (*e.g.* for image-guided drug delivery). Herein, we report on the preparation and characterization of DTX-loaded BCMs, using the biocompatible and biodegradable PEG-*b*-PCL copolymer (Hoang et al., 2012; Liu et al., 2007) decorated with pyrazolyl-diamine chelating units to stabilize the organometallic core *fac*-[M$(CO)_3]^+$ (M = Re, ^{99m}Tc). The anti-proliferative properties of the BCMs, the cellular uptake of ^{99m}Tc-BCMs in selected human cancer cell lines and a preliminary *in vivo* evaluation are also presented and discussed.

2. Experimental procedures

2.1. Materials

Unless otherwise stated, all chemicals and solvents were of reagent grade and used without further purification. Poly(ethylene glycol) methyl ether (Me-PEG, M_n = 5000), from Sigma-Aldrich, and *O*-(2-Aminoethyl)polyethylene glycol (NH2-PEG, M_n = 3000), from Fluka, were dried twice by azeotropic distillation in toluene that was distilled off completely. Sigma-Aldrich ε-caprolactone (CL) was dried using calcium hydride and distilled prior to use. Sigma-Aldrich dichloromethane was dried by phosphorus pentoxide. Dried toluene, from Fisher Chemical, was obtained by distillation with sodium. *N,N'*-Dicyclohexylcarbodiimide (DCC), N-hydroxysuccinimide (NHS), hydrogen chloride solution 2 M in diethyl ether and pyrene, were all acquired from Sigma-Aldrich. Docetaxel anhydrous (DTX) was purchased from Chemos GmbH.

2.2. Methods

^{1}H NMR spectra were recorded in a Bruker AVANCE II 300 or 400 MHz instruments. Chemical shifts of ^{1}H (δ, ppm) are reported relative to the residual solvent peaks relative to $SiMe_4$. Infrared spectra were recorded as KBr pellets on a Bruker, Tensor 27 spectrometer. HPLC analysis was performed on a Perkin-Elmer LC pump 200 coupled to a LC tunable UV–vis detector (227 nm) and to a γ detector (Berthold LB 509). The solvents were of HPLC grade. DTX analysis was performed with a EC 250/4 mm (L/ID) Nucleosil 100-10 C18 column and a isocratic method using acetonitrile and trifluoroacetic acid (TFA) 0.1% aqueous (50/50, v/v) as the mobile phase with a flow rate of 1 mL/min for 15 min. DTX was quantified with reference to a calibration curve. Radiolabeled micelles were analyzed by size-exclusion chromatography using a TSKgel G3000 SW 7.5 mm × 30 cm (IDxL) column with a particle size of 10 μm and a pore size of 250 Å coupled to a pre-column TSKgel SW Guard column 7.5 mm IDx7.5 cm with a particle size of 10 μm using as mobile phase 0.1 M phosphate buffer with 0.1 M Na_2SO_4 (pH = 6), with a flow rate of 1.0 mL/min for 30 min. The radiolabeled copolymers and micelles were also analyzed by ITLC-SG (Glass Microfibre Chromatography Paper impregnated with silica gel) using as mobile phase: 1) methanol/6N HCl (95/5, v/v); 2) 0.9% saline/methanol (95/5, v/v). Fluorescence spectra were measured on Horiba Jobin Yvon fluorescence spectrometer model FL 1065 at room temperature with quartz suprasil fluorescence cuvettes.

2.3. Synthesis and characterization of copolymers

Copolymers methoxy-terminated poly(ethylene glycol)-*b*-poly (ε-caprolactone) (Me-PEG-*b*-PCL) and amino-terminated poly (ethylene glycol)-*b*-poly(ε-caprolactone) (NH_2-PEG-*b*-PCL) were synthesized by metal-free cationic ring-opening polymerization of ε-caprolactone (ε-CL) *via* an activated monomer mechanism with HCl-diethyl ether (Liu et al., 2007) using methoxy-terminated poly (ethylene glycol) (HO-PEG-CH_3) and amino-terminated poly (ethylene glycol) (HO-PEG-NH_2) as macroinitiators, respectively. The reaction mixture was stirred overnight and then was slowly poured into cold (4° C) diethyl ether to precipitate the copolymer that was recovered by filtration as previously described (Kim et al., 2005; Lou et al., 2002; Zeng et al., 2006).

2.3.1. Synthesis and characterization of Pz-PEG-b-PCL

The bifunctional pyrazolyl-diamine chelator (Pz) and the corresponding Boc-protected chelator, Pz(Boc), (4-((2-(tert-butoxycarbonylamino)ethyl)(2-(3,5-dimethyl-1H-pyrazol-1-yl)ethyl) amino)butanoic acid), were synthesized and characterized as previously reported (Alves et al., 2005).

The activation of the free carboxylic group in the Boc-protected prochelator, Pz(Boc), and posterior conjugation to NH_2-PEG-*b*-PCL was based on Yang X. et al. work (Yang et al., 2008; Zeng et al., 2006). The carboxylic group was activated by dissolving Pz-Boc (258 mg, 0.7 mmol), DCC (217 mg, 1.05 mmol) and NHS (121 mg, 1.05 mmol) in 20 mL of dried CH_2Cl_2. After overnight, the mixture was filtered to remove the precipitated (dicyclohexylurea (DCU)) and dried under vacuum. Then, the activated pro-chelator, NHS-Pz (Boc), was added in 5 molar excess, considering that activation yield was 100%) to a stirred mixture of NH_2-PEG-*b*-PCL (1.40 g, 0.14 mol) and triethylamine (0.10 mL, 0.7 mmol) in dried CH_2Cl_2 (5 mL). After 24 h at room temperature (RT), the copolymer was obtained as described above for Me-PEG-*b*-PCL and NH_2-PEG-*b*-PCL.

Lastly, the Pz(Boc)-PEG-*b*-PCL was dissolved in a small volume of CH_2Cl_2 (V = 3 mL) and a large excess of TFA (0.3 mL) was added to remove the Boc protecting group (Alves et al., 2005). The reaction mixture was maintained overnight under stirring at RT, the solvent was evaporated and the residue washed with CH_2Cl_2 (3 times), to afford Pz-PEG-*b*-PCL.

Pz-PEG-*b*-PCL ^{1}H NMR ($CDCl_3$, δ ppm): signals for PCL appeared at 1.36 (CO-CH_2-CH_2-CH_2-CH_2-O), 1.63 (CO-CH_2-CH_2-CH_2-CH_2-CH_2-O), 2.28 (CO-CH_2-CH_2-CH_2-CH_2-CH_2-O) and 4.06 (CO-CH_2-CH_2-CH_2-CH_2-CH_2-O), whereas the peaks at 3.58 (4H, –O-CH_2-CH_2-) and 4.20 (O-CH_2-CH_2-O-CO) were assigned to the PEG block and the signal at 5.91 correspond to H(4)-pz and 1.88 to methyls-pz. **IR (KBr) (ν/cm^{-1}):** 3452 cm^{-1} (—OH, stretching vibration, PCL), 2945 cm^{-1} (C—H, stretching vibration, PCL), 2868 cm^{-1} (C—H, stretching vibration, PEG), 1726 cm^{-1} (C=O, stretching vibration, PCL), 1630 cm^{-1} (C=O, bending vibrations, amide bond), 1574 cm^{-1} (N—H, bending vibrations, NH_2)

1471 cm^{-1}, 1420 cm^{-1}, 1399 cm^{-1} and 1368 cm^{-1} (C—N and C—O—H, polymer backbone) and 1193 cm^{-1} and 1171 cm^{-1} (O—C—O and C—O, polymer backbone).

2.4. Preparation of micelles

Me-BCMs and Me(DTX)-BCMs were synthesized by the thin-film hydration method (Hoang et al., 2012). Briefly, Me-PEG-*b*-PCL (50 mg, 5 μmol) and DTX (only for the loaded micelles (2.3 mg, 2.8 μmol)) were dissolved in DMF and maintained 4 h under stirring at RT. Then, the solvent was evaporated slowly under N_2 to form the DTX/Me-PEG-*b*-PCL thin-film, which was then hydrated at 60 °C with PB (phosphate buffer 0.01 M pH 7.4) and stirred for 4 h at RT. The micelles were purified by dialysis using Spectra/Por(R) 6 regenerated cellulose dialysis membrane with a molecular weight cut-off (MWCO) of 25,000 Da. Water with 5% of methanol was used as dialysis medium to enhance the solubility of non-encapsulated DTX and amphiphilic copolymers. After 24 h the micelles were recovered and lyophilized.

Functionalized micelles were obtained by the incorporation of Pz-PEG-*b*-PCL through the transfer method (Hoang et al., 2012; Zeng et al., 2006). Briefly, 400 μL of Pz-PEG-*b*-PCL (1.25×10^{-4} M) in PB were added to 2 mL of Me-BCMs or Me(DTX)BCMs in a concentration of 1 g/L. The mixture was maintained under stirring for 1 h at 60 °C and then overnight at RT to obtain Me/Pz-BCMs and Me/Pz(DTX)BCMs, respectively. The functionalized micelles were then lyophilized.

Pz-BCMs and Pz(DTX)BCMs were obtained using the procedure described above for Me-BCMs and Me(DTX)BCMs and using the copolymer Pz-PEG-*b*-PCL.

2.5. Size, zeta potential and morphology of micelles

The hydrodynamic diameter (D_h), and zeta potential of micelles (0.1 g/L) were determined in 0.01 M phosphate buffer (PB) pH 7.4, using a Zetasizer Nano ZS from Malvern with zeta-potential cells. The particle size was measured by dynamic light scattering (DLS) at 25 °C with a 173° scattering angle, and an optic arrangement known as non-invasive back scatter (NIBS). Measurements were repeated three times. The shape and morphology was observed by transmission electron microscopy (TEM) with a Hitachi H-8100 electron microscope operating at 500 keV. Micelles dissolved in 0.01 M PB, pH 7.4 at 0.1 g/L were placed on negatively charged carbon-coated copper grids and left to dry at RT.

Before using, all the micelles were dissolved in 0.01 M phosphate buffer, pH7.4 (PB) in order to obtain 1 g/L solutions that were subsequently sonicated for 20 min. Then, the solutions were diluted and filtered using a 0.20 μm syringe filter. For stability studies the micelles solution (1 g/L) were left at 37 °C and aliquots were analyzed by DLS at different time points (0, 1, 4 and 7 days incubation time).

2.6. Critical micelle concentration

The critical micelle concentration (CMC) for Me-PEG-*b*-PCL and Pz-PEG-*b*-PCL copolymers was determined by an established fluorescence-based method (Zhang et al., 1996) using pyrene as the fluorescent probe since its fluorescence intensity changes according to the polarity surrounding the pyrene molecules (Goncalves et al., 2007; Topel et al., 2013). Aliquots of Me-PEG-*b*-PCL or Pz-PEG-*b*-PCL in $CHCl_3$ with increasing concentrations (0.1–100 mg/L) were prepared. Subsequently, an aliquot of pyrene was added to each vial keeping the pyrene at a concentration of 1×10^{-6} M. After stir ring the different solutions for 4 h, the solvent was evaporated under nitrogen. The vials were then heated to 60 °C and 1 mL of distilled water was added to each vial and the mixture stirred overnight at room temperature. Emission fluorescence spectra were recorded in the range 350–500 nm, after excitation at 337 nm with a spectrofluorimeter Horiba Jobin Yvon with excitation and emission slits of 3 nm. The ratio of the peak intensities at 373 nm (I_1) and at 383 nm (I_3) were determined for each emission spectra and represented as a function of the copolymer concentration. The CMC value corresponds to the intersection of the best fit lines (Goncalves et al., 2007; Topel et al., 2013).

2.7. DTX loading content

The DTX loading content (LC) and DTX loading efficiency (LE) were determined by RP-HPLC with reference to a standard calibration curve. Briefly, 4 mg of loaded BCMs were dissolved in 500 μL of acetonitrile, sonicated and centrifuged at 3000*g* for 10 min to precipitate the copolymer. The supernatant was collect and analyzed by HPLC at 227 nm.

The LC was calculated by the ratio of entrapped DTX over the total amount of micelles and LE was calculated as the ratio of entrapped DTX over the total amount of DTX used to prepare the respective micelles (Hoang et al., 2012).

2.8. In vitro *DTX release study*

In vitro release of DTX from Me(DTX)BCMs was evaluated at pH 7.4 and 5.0 using the dialysis method (Hoang et al., 2012; Liu et al., 2011; Muthu et al., 2015). Briefly, solutions of Me(DTX)BCMs in 0.01 M phosphate buffer, pH 7.4 were placed in a regenerated cellulose tubular dialysis membrane (MWCO = 6000–8000 Da) and subsequently immersed into 30 mL of phosphate buffer 0.01 M (pH 7.4 or pH 5.0) containing 0.5% Tween 80 (w/v) to enhance the solubility of DTX. Dialysis occurred at 37 °C under continuous stirring. At certain time intervals, the dialysis membrane with the Me(DTX)BCMs was taken out and immediately immersed into new containers with fresh medium. The amount of DTX in each dialysis medium and in each dialysate was determined by RP-HPLC (see above). The drug release profiles were calculated as the accumulative percentage of released DTX *versus* time and the 100% release correspond to the total amount of DTX entrapped in the micelles. As a control, the release profile of free DTX was also evaluated using the same experimental conditions.

2.9. Anti-proliferative activity

The anti-proliferative activity of the micelles was performed in human tumor cell lines, namely: breast cancer cell line MDA-MB-231, prostate cancer cell line PC3 and osteosarcoma cell line MNNG HOS (ATCC). The cells were cultured in DMEM + GlutaMAX- I (MDA-MB-231 and MNNG HOS) or RPMI (PC3) and seeded at a density of 1.5×10^4 cells/cm^2 (MDA-MB-231 and MNNG HOS) and 2.0×10^4 cells/cm^2 (PC3) in 96-well plates. Cells were allowed to adhere for 24 h, cultured in standard conditions. After 48 h exposure to the different micelles, Alamar Blue (1:20) (Life-Technologies) was added to each well. Cells were incubated for 2.5 h at 37 °C and 5% CO_2, and fluorescence was measured in an Infinite 200 Plate Reader (Tecan) (excitation 560 nm, emission 590 nm). Fluorescence intensity was measured and the results were expressed in% of cell viability.

2.10. Micelles labeling with fac-$[^{99m}Tc(CO)_3]^+$

Na[$^{99m}TcO_4$] was eluted from a $^{99}Mo/^{99m}Tc$ generator, using 0.9% saline. IsoLink® kit was used to prepare the radioactive precursor *fac*-[$^{99m}Tc(CO)_3(H_2O)_3]^+$ as described in the literature (Alberto et al., 2001).

The micelles were radiolabeled with *fac*-[^{99m}Tc(CO)$_3$]$^+$ using two different methods: in the direct method the functionalized micelles were radiolabeled with *fac*-[^{99m}Tc(CO)$_3$]$^+$, while in the indirect method the functionalized copolymer was previously radiolabeled and used to prepare the radiolabeled micelles. In the direct method, 400 μL of the precursor *fac*-[^{99m}Tc(CO)$_3$(H$_2$O)$_3$]$^+$ was added to 200 μL of functionalized micelles (1 g) and the reaction mixture was incubated at 60 °C for 90 min. In the indirect method, 100 μL of Pz-PEG-*b*-PCL (1.25×10^{-4} M) reacted with 900 μL of *fac*-[^{99m}Tc(CO)$_3$(H$_2$O)$_3$]$^+$ for 30 min at 100 °C. Then,

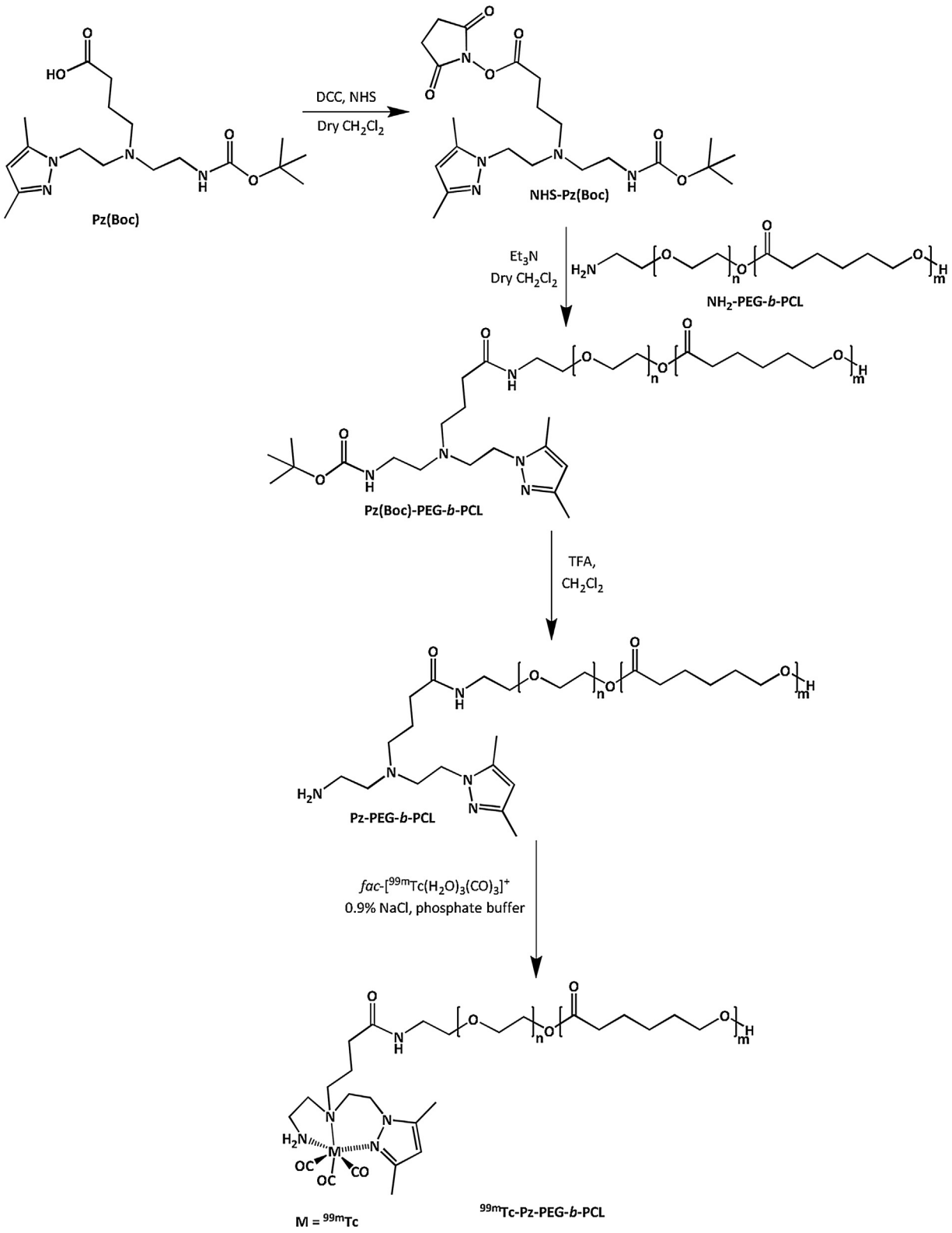

Fig. 1. Synthesis of ^{99m}Tc-Pz-PEG-*b*-PCL.

250 μL of radiolabeled Pz-PEG-*b*-PCL was added to 200 μL of Me-BCMs or Me(DTX)BCMs (1.0×10^{-4} M) and the reaction mixture was left at 60 °C for 1 h. In both methods, the ^{99m}Tc(I)-micelles were purified using 10 kDa Amicon centrifugal filters (Guo et al., 2013). The radiochemical labeling yield as well as the radiochemical purity of the labeled micelles were determined by GPC-HPLC and ITLC-SG using the methods described above. The *in vitro* stability was evaluated at 37 °C in PB (pH 7.4, 0.01 M) and in cell culture medium (Dulbecco's modified Eagle's medium, DMEM).

For control, the bifunctional chelator Pz-NN was radiolabeled as described in the literature (Alves et al., 2005) and a similar procedure was used to radiolabel the copolymer NH_2-PEG-*b*-PCL.

2.11. Cellular uptake

The cellular uptake experiments were performed with the same cell lines used in the anti-proliferative studies. The cells were cultured in DMEM + GlutaMAX- I (MDA-MB-231 and MNNG HOS) or RPMI (PC3) media and seeded at a density of 2.5×10^5 cells/500 μL in 24-well plates. Cells were allowed to adhere for 24 h and then were incubated with ~37 kBq/0.5 mL (~1 μCi/0.5 mL) of the radiolabeled BCMs (Me/Pz-BCMs or Me/Pz(DTX)BCMs) in media at 37 °C for different time points 0.5 h–17 h. Incubation was ended by washing the cells with ice-cold medium followed by a two wash steps with cold PB. Then, the cells were lysed by 15 min incubation with 1 M NaOH at 37 °C to assess the cellular associated radioactivity. The radioactivity in the medium and in the cells were separately, collected and counted in a γ counter. Cellular uptake data was based on three determinations for each time point and are expressed as mean ± SD.

2.12. Biodistribution

The biodistribution profile of the ^{99m}Tc-Me/Pz(DTX)BCMs was evaluated in groups of healthy female BALB/c mice (Charles River, France) weighting between 16 and 25 g each. Animals were intravenously injected with 100 μL (8.5–16.0 MBq) of each preparation *via* the tail vein and were maintained on normal diet *ad libitum*. At 4 h and 24 h post-injection (*p.i.*) mice were sacrificed by cervical dislocation. The biodistribution profile of the radiolabeled copolymer ^{99m}Tc-Pz-PEG-*b*-PCL was also evaluated at 1 h, 4 h and 24 h *p.i.* The radioactive administered dose and the radioactivity in the sacrificed animal were measured in a dose calibrator (Capintec CRC25R). The difference between the radioactivity in the injected and sacrificed animal was assumed to be due to excretion. Blood samples were taken by cardiac puncture at sacrifice. Tissue samples of the main organs were then removed, weighted and counted in a gamma counter (LB2111, Berthold, Germany). The uptake in the organs/tissues was calculated and expressed as a percentage of the injected activity per gram (%I.A./g).

All animal experiments were performed in accordance with the guidelines for animal care and ethics for animal experiments outlined in the National and European Law.

2.13. Statistical analysis

Values are expressed as means and the error bars in graphs represent the standard error of the means (SEM). All statistical comparisons were done with the GraphPad Prism 6.0 software for Windows (GraphPad software). Multiple comparison of means was done with the one-way ANOVA test, using Dunnett's multiple comparison test. To exclude experimental outliers, Grubbs' test was used. The level of statistical significance was set at $p < 0.05$. $^{*}p < 0.05$, $^{**}p < 0.01$, $^{***}p < 0.001$ and $^{****}p < 0.0001$.

3. Results and discussion

3.1. Synthesis and characterization of copolymers

The diblock copolymers Me-PEG-*b*-PCL and NH_2-PEG-*b*-PCL were synthesized by metal-free cationic ring-opening polymerization of ε-caprolactone (CL) *via* an activated monomer mechanism with HCl-diethyl ether, following reported synthetic methodologies (Liu et al., 2007). The copolymers were characterized by ^{1}H NMR and FTIR spectroscopy, with the spectroscopic data collected being similar to those described in the literature (Hoang et al., 2009; Kim et al., 2005; Liu et al., 2007). For NH_2-PEG-*b*-PCL, the absence in the ^{1}H NMR spectrum of a resonance in the amide bond region indicated that polymerization has not taken place through the terminal amine group of NH_2-PEG, but *via* the hydroxyl end group of the polymer (Hoang et al., 2009). The pyrazolyl-diamine chelating unit with a *N*,*N*,*N*-donor atom set was selected as it gives highly stable $M(CO)_3$ complexes (M = Re, ^{99m}Tc), allowing the radiolabeling and biological evaluation of a wide variety of molecular and nanostructures bearing or not relevant biomolecules (Alves et al., 2005; Correia et al., 2011; Morais et al., 2011; Raposinho et al., 2010). Conjugation of NH_2-PEG-*b*-PCL to the NHS–activated bifunctional chelator under basic conditions afforded the intermediate polymer (Boc)Pz-PEG-*b*-PCL. Precipitation with cold ether, followed by treatment with trifluoracetic acid led to the final block copolymer derivative (Pz-PEG-*b*-PCL) functionalized with the pyrazolyl-diamine chelator for radiolabeling with ^{99m}Tc(I) (Fig. 1). The ^{1}H NMR spectrum of the copolymer Pz-PEG-*b*-PCL displayed a characteristic singlet at δ 5.91 ppm, assigned to the H(4) proton of the azolyl ring, (Morais et al., 2011) (Fig. S1, Supplementary material) and the FTIR spectrum showed a new band at 1630 cm^{-1} due to ν(C=O) stretching band of the amide bond. The conjugation of the bifunctional chelator to the copolymer was also confirmed indirectly by radiolabeling Pz-PEG-*b*-PCL (Fig. 1) and NH_2-PEG-*b*-PCL with *fac*-$[^{99m}Tc(H_2O)_3(CO)_3]^+$, and by comparing the labeling yield and the stability of the resulting radiolabeled nanocompounds. Indeed, in the case of the copolymer NH_2-PEG-*b*-PCL, the radiolabeled derivative ^{99m}Tc-NH_2-PEG-*b*-PCL was obtained in very low yield (<10%) and presented very low stability, whereas the labeling of Pz-PEG-*b*-PCL led to the radiolabeled compound ^{99m}Tc-Pz-PEG-*b*-PCL in almost quantitative yield (>95%), a species highly stable *in vitro*. The high ability of the pyrazolyl-diamine chelating unit to stabilize the organometallic unit *fac*-$[M(CO)_3]^+$ (M = ^{99m}Tc, Re) and the high *in vitro* and *in vivo* stability of the resulting metallated conjugates has already been thoroughly demonstrated (Alves et al., 2005; Correia et al., 2011; Raposinho et al., 2010).

The chemical composition and molecular weight of the copolymers were calculated based on the intensity ratio of the methylenic peak of the PEG block (at δ 4.20) and the resonance of the PCL block (at δ 2.28) and on the known molecular weight of the PEG precursor. Taking the calculated number of CL monomers, which was similar (ca. 45) for Me-PEG-*b*-PCL and NH_2-PEG-*b*-PCL, the estimated molecular weight for Me-PEG-*b*-PCL, NH_2-PEG-*b*-PCL and Pz-PEG-*b*-PCL was 10,000 Da, 8000 Da and 8400 Da, respectively.

3.2. Size, zeta potential and morphology of micelles

The non-loaded (Me-BCMs and Pz-BCMs) and DTX-loaded micelles (Me(DTX)BCMs and Pz(DTX)BCMs) were prepared by the thin-film hydration method, (Hoang et al., 2012) using the block copolymers described above. The mixed micelles Me/Pz-BCMs and Me/Pz(DTX)BCMs were prepared upon incorporation of the copolymer Pz-PEG-*b*-PCL into the respective precursors Me-BCMs

Table 1
Hydrodynamic diameter (D_h), Zeta Potential and DTX Loading Content (LC) of Micelles.

Micelles	Size (nm)		PDI	Zeta potential (mV)	LC (%)
	TEM[a]	D_h[b]			
Me-BCMs	41.8 ± 5.2	59.5 ± 4.6	0.26 ± 0.01	−1.4 ± 0.8	–
Me(DTX)BCMs	30.5 ± 8.0	39.0 ± 4.6	0.42 ± 0.01	−1.8 ± 1.2	3.2 ± 0.3
Me/Pz-BCMs	40.6 ± 16.4	35.5 ± 4.7	0.48 ± 0.06	−2.1 ± 0.4	–
Me/Pz(DTX)BCMs	42.8 ± 15.6	58.6 ± 7.8	0.36 ± 0.01	−4.5 ± 2.3	0.55 ± 0.05
Pz-BCMs	38.0 ± 7.1	66.5 ± 5.2	0.41 ± 0.10	−4.6 ± 1.0	–
Pz(DTX)BCMs	14.9 ± 1.7	55.7 ± 12.4	0.25 ± 0.05	−8.4 ± 4.2	2.1 ± 0.1

[a] Micelle surface area was calculated by IMAGEJ image processing software.
[b] Mean±SD of distribution by number (refractive index = 1.5).

or Me(DTX)BCMs, using the transfer method described elsewhere (Hoang et al., 2012; Zeng et al., 2006).

The relative hydrodynamic diameter (D_h) and the zeta potential of the BCMs were determined by dynamic light scattering (DLS) (Table 1) and the morphology was evaluated by transmission electron microscopy (TEM). As an example, Fig. 2 displays a DLS histogram and a TEM image for Me/Pz(DTX)BCMs.

The DLS measurements showed that the majority of the BCM's had a monomodal size distribution and that the D_h are all of the same order of magnitude, varying between 35.5 ± 4.7 nm (Me/Pz-BCMs) and 66.5 ± 5.2 nm (Pz-BCMs). As can be seen in Table 1, within the measurement uncertainty the average hydrodynamic diameters (D_h) found for loaded and non-loaded micelles as well as for functionalized and non-functionalized micelles do not allow to establish any trend. The analysis by TEM revealed a spherical morphology and a relatively uniform size distribution as can be observed in the example in Fig. 2. Additionally, the size calculated by TEM correlate well with D_h determined by DLS (Table 1) except for the micelles prepared without Me-PEG-bPCL where a relatively lower size was found by TEM.

Moreover, the DLS measurements have also shown a very high stability (up to 7 days in 0.01 M phosphate buffer pH 7.4 at 37 °C) for Me-BCMs, Me(DTX)BCMs, Me/Pz-BCMs and Me/Pz(DTX)BCMs.

The zeta potential values found for the micelles in phosphate buffer vary between −1.4 ± 0.8 mV (Me-BCMs) and −8.4 ± 4.2 mV (Pz(DTX)BCMs). The values found for the DTX-loaded micelles described in this work are within the zeta potential range of −10 mV to +10 mV, considered promising for a long circulation time, low serum protein aggregation and low MPS clearance, all important parameters for passive targeting (Ernsting et al., 2013; Hoang et al., 2009; Li and Huang, 2008; Torchilin, 2007).

3.3. Critical micelle concentration

Critical micelle concentration (CMC) can be defined as the minimal concentration at which amphiphilic copolymer chains are thermodynamically driven to self-assemble in aqueous solution forming micelles. CMC is a very important parameter in micelle formation and on their thermodynamic stability. In general, micelles that are formed at low CMC are more stable *in vivo,* even after diluted in the bloodstream (Allen et al., 1999; Lee et al., 2005). In this work, the CMC was determined by a very sensitive and well-established fluorescence-based method (Fig. S2). Pyrene was used as a fluorescent probe since its properties change when encapsulated by the micelles, *i.e.*, when transferred from the aqueous to the hydrophobic environment (Goncalves et al., 2007; Topel et al., 2013). The I_3/I_1 ratio was used to determine the CMC value by fluorescence (Fig. S2, right) (Kim et al., 2005). The CMC for the copolymer Me-PEG-*b*-PCL was 4 mg/L, comparable with the ones found for similar BCMs described in the literature (Lee et al., 2010; Liu et al., 2007; Mikhail et al., 2014), whereas for the new copolymer Pz-PEG-*b*-PCL the CMC found was higher (65 mg/L).

3.4. Drug loading content

The DTX loading content (LC) and DTX loading efficiency (LE) were determined by HPLC with reference to a standard calibration curve as described in the experimental section. The LC is the ratio of the entrapped DTX in the micelles over the total amount of loaded micelles, while LE is the total amount of the DTX in the micelles and is found by the ratio of entrapped DTX over the total amount of DTX used to prepare the respective BCMs (Hoang et al., 2012).

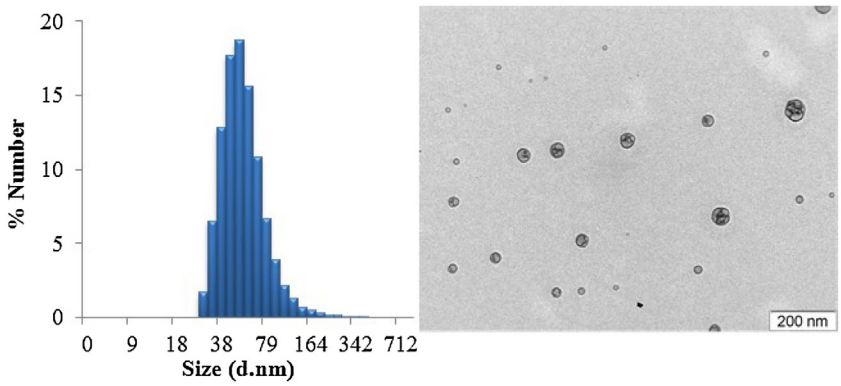

Fig. 2. DLS histogram and TEM image of Me/Pz(DTX)BCMs.

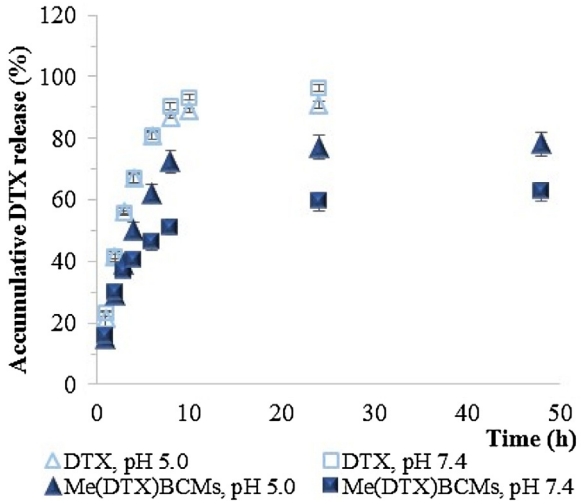

Fig. 3. *In vitro* DTX release profile from Me(DTX)BCMs and DTX solution at pH 7.4 and 5.0. Data are presented as mean ± SD.

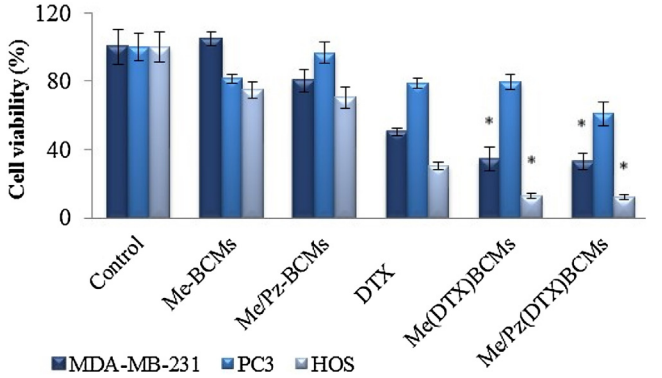

Fig. 5. Anti-proliferative study for DTX loaded micelles on MDA-MB-231 breast, PC3 prostate and MNNG HOS osteosarcoma cancer cells at 48 h of incubation, comparing with DTX. When present, DTX concentration was 2 nM and the concentration of the non-loaded micelles was the same used for the corresponding loaded micelles. *$p < 0.05$, comparing with free DTX.

The LC and LE depend on the copolymer used in the thin-film method for the preparation of the corresponding BCMs. For Me(DTX)BCMs, formed by the copolymer Me-PEG-*b*-PCL, the drug LC was 3.2 ± 0.3% and the LE was 63 ± 10%. For Pz(DTX)BCMs, the DTX LC and LE decreased to 2.1 ± 0.1% and 23 ± 0.7%, respectively. For the mixed micelles Me/Pz(DTX)BCMs, the drug LC decrease to 0.55 ± 0.05% due to the addition of a new copolymer.

3.5. *DTX release* in vitro

The *in vitro* release of DTX from Me(DTX)BCMs was assessed by dialysis at physiological pH (pH 7.4) and in slightly acidic conditions (pH 5.0). As can be seen in Fig. 3, the DTX showed a fast initial release followed by a sustained one. The release profile is comparable to other micelles also prepared from PEG-*b*-PCL type copolymer loaded with DTX or with other cytotoxic agents (Diao et al., 2011; Liu et al., 2011; Mikhail et al., 2013; Palma et al., 2014). A higher DTX release was observed by Mikhai A.S. and Allen C., using PEG-*b*-PCL micelles at 8 h of dialysis (~40% higher). Such difference may be due to the longer hydrophobic chain of our copolymer (5000 g/mol) compared to the one used by the authors (2000 g/mol) since a longer chain may promote a lower DTX diffusion (Mikhail and Allen, 2010).

The drug content release at different time points is dependent on the pH, with a higher release at pH 5.0. Indeed, after 8 h, 72% of the loaded DTX was released at pH 5, whereas only 51% has been released at pH 7.4 (Fig. 3). As a control, we have also evaluated the DTX release to the dialysis medium using a similar amount of free DTX (pH 7.4 and 5.0). In this case, the release is not pH dependent and is considerably faster in comparison to the entrapped DTX in the micelles, especially for pH 7.4. In fact, after 8 h of dialysis around 90% of DTX was already released for both pH values (Fig. 3). As the loaded BCMs were stable in 0.01 M phosphate buffer pH 7.4 at 37 °C for 7 days, the DTX release observed at pH 7.4 probably occurs predominantly by diffusion (Mikhail and Allen, 2010). The higher release observed at pH 5.0 could be related with the cleavage of the ester bonds present in the caprolactone polymer, which are acid-labile chemical bonds (Liu et al., 2014) and consequently lead to higher micelles' degradation at this pH value. The pH in primary and metastasized tumors as well as in their microenvironment is lower (pH 5.0) than in the blood stream or in the normal tissues (Manchun et al., 2012). Consequently, the higher DTX release found at pH 5.0 is a favorable behavior for cancer therapy since it could increase the therapeutic effect with less side effects (Guo et al., 2013).

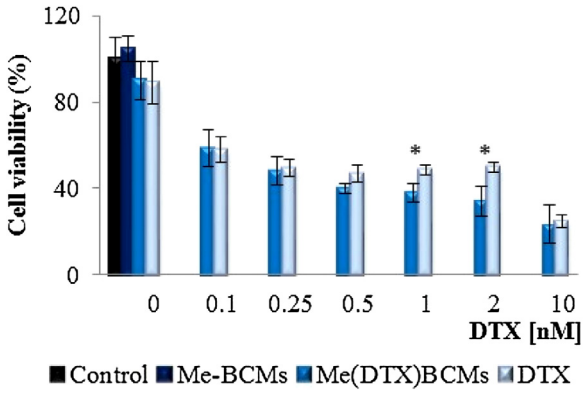

Fig. 4. DTX concentration (0.1–10 nM) effect on cell viability studies of DTX and DTX loaded micelles (Me(DTX)BCMs) on MDA-MB-231 breast cancer cell line at 48 h of incubation. The Me-BCMs concentration (for DTX = 0 nM) was the same concentration used to obtain 2 nM of DTX. *$p < 0.05$, comparing with free DTX.

3.6. *Anti-proliferative activity*

The anti-proliferative activity of non-loaded and DTX-loaded micelles (Me-BCMs, Me(DTX)BCMs, Me/Pz-BCMs and Me/Pz(DTX)BCMs) was assessed by the Alamar Blue assay in different human cancer cell lines, and compared with that of free DTX. First, we performed a preliminary study in which the anti-proliferative effect of DTX and DTX-loaded micelles (Me(DTX)BCMs) was assessed in MDA-MB-231 breast cancer cells at 48 h incubation time. In the tested concentration range (0.1–10 nM), the results showed a concentration dependent anti-proliferative effect (Fig. 4).

Next, we assessed the anti-proliferative activity of functionalized micelles at 2 nM DTX concentration (Fig. 5). As expected, the non-loaded micelles (Me-BCMs and Me/Pz-BCMs) did not presented considerable anti-proliferative activity. On the contrary, in the case of the DTX-loaded micelles (Me(DTX)BCMs and Me/Pz(DTX)BCMs), the anti-proliferative effect was dependent upon the cell type and time of incubation. Entrapment of the DTX improved

significantly the anti-proliferative effect over MDA-MB-231 and MNNG HOS cells, with a decrease in the cell viability of 1.5 and 2.3-fold, respectively. For the PC3 cells the anti-proliferative effect was lower than that observed for the other two cancer cell lines. This prostate cell line (androgen independent prostate cells) has been described as resistant cells to chemotherapeutic agents. The mechanism of resistance often associated with an increased efflux of the drugs could result in a decreased uptake. Moreover, the uptake is energy-dependent *i.e.*, dependent on the glycolytic flux involving ATP production and in these cells the ATP formation is lower due to higher ATPase activity (Ronquist et al., 2016; Vaz et al., 2012). Considering that the uptake and the anti-proliferative effect are associated, the higher cellular viability observed for the PC3 cells may be related with their glycolytic profile. This is in agreement with the results obtained in the cellular uptake studies since the PC3 cells presented the lowest uptake values (see below).

For all the cell lines, the anti-proliferative effect was more pronounced when using the functionalized micelles (Me/Pz(DTX) BCMs). In comparison to the free DTX, the loaded-micelles require lower DTX concentration and thus can induce a similar therapeutic effect with reduced side effects.

3.7. ^{99m}Tc-BCMs

All pyrazolyl-diamine(Pz)-containing micelles were labeled directly by incubation with the organometallic precursor *fac*-$[^{99m}Tc(CO)_3(H_2O)_3]^+$ (90 min, at 60 °C). Additionally, the mixed micelles Me/Pz-BCMs and Me/Pz(DTX)BCMs were also labeled by an indirect method, in which the copolymer Pz-PEG-*b*-PCL was first radiolabeled (30 min, 100 °C, $\eta > 95\%$) with the same precursor and then incorporated into the micelles by a modified version of the above described transfer method. In the latter procedure, due to the half-life of ^{99m}Tc (6 h), the overnight stirring at RT and lyophilization could not be performed as in the original method. The overall radiochemical yield was lower (ca. 65%), when compared to the direct method, possibly due to higher unspecific retention of ^{99m}Tc-Pz-PEG-*b*-PCL in the Amicon filters used for purification. Nevertheless, in both methods after purification by ultrafiltration (Ultra Centrifugal filters (Amicon filters)) the radiolabeled micelles were obtained with high radiochemical purity (>95%). The radiochemical yield and purity were determined by GPC-HPLC and ITLC-SG (Fig. S3, Supplementary material). The stability of the radiolabeled micelles, prepared by the direct or indirect method, was evaluated in 0.01 M PB pH 7.4 at 37 °C for 3 h (Fig. 6). These results showed that only the radiolabeled micelles obtained by the direct method, ^{99m}Tc-Me/Pz-BCMs and ^{99m}Tc-Me/Pz(DTX)BCMs, were stable under physiological conditions (pH 7.4, 37 °C). Moreover, these micelles are also stable in the cell culture medium (DMEM), and in 0.01 M PB pH 7.4, at 37 °C for 18 h (Fig. S4, Supplementary material). Hence, in the indirect method the overnight stirring at room temperature seems to be essential for the micelles stability since Hoang, B. et al. obtained stable micelles using similar conditions with overnight stirring (Hoang et al., 2012). Moreover, the preparation of micelles with the copolymer Me-PEG-*b*-PCL and its posterior functionalization by the transfer method seems to be fundamental to get stable micelles.

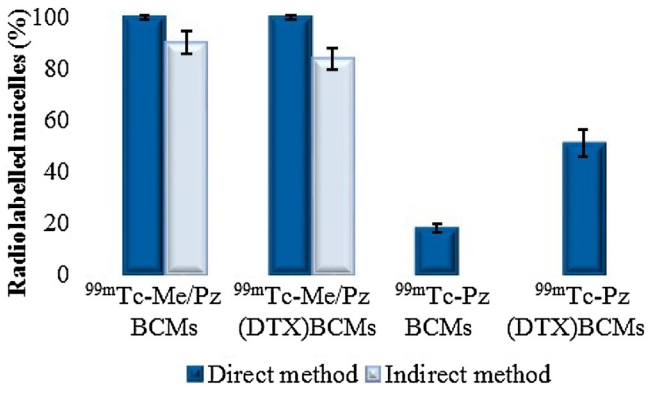

Fig. 6. Stability of the radiolabeled micelles in 0.01 M PB pH7.4, for 3 h, at 37 °C.

3.8. Cell uptake studies

Uptake kinetic studies in the MDA-MB-231, PC3 and MNNG HOS cells were performed with the radiolabeled micelles ^{99m}Tc-Me/Pz-BCMs and ^{99m}Tc-Me/Pz(DTX)BCMs and also with the precursor *fac*-$[^{99m}Tc(CO)_3(H_2O)_3]^+$ in the MDA-MB-231 cells for comparison (Fig. 7).

The labeled micelles presented relevant higher uptake than the precursor fac-$[^{99m}Tc(CO)_3(H_2O)_3]^+$. For the three cell types similar trends were observed for the radiolabeled micelles: rapid uptake up to 4 h of incubation followed by a relatively steady phase

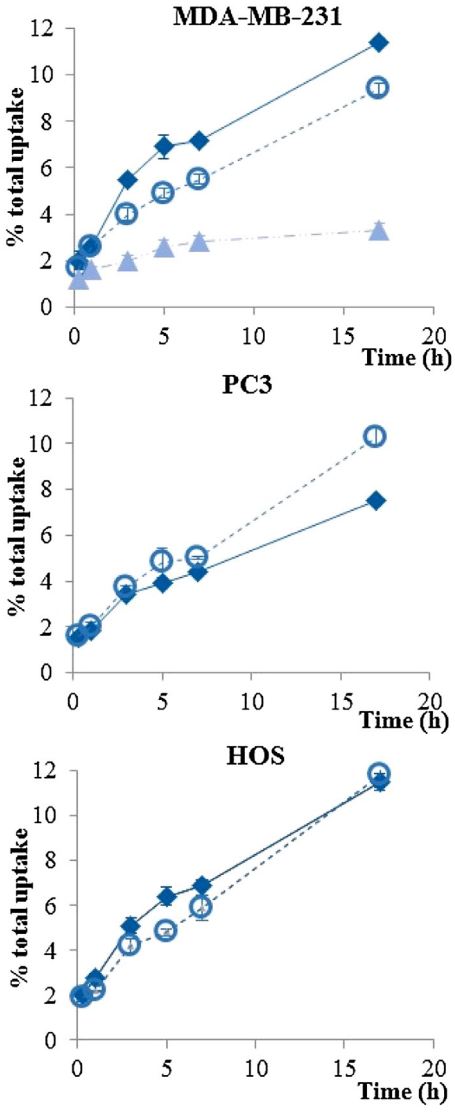

Fig. 7. Cellular uptake of ^{99m}Tc-Me/Pz-BCMs (○) and ^{99m}Tc-Me/Pz(DTX)BCMs (◆) and *fac*-$[^{99m}Tc(CO)_3(H_2O)_3]^+$ (▲) in MDA-MB-231, PC3 and MNNG HOS cells lines.

between 4 h and 7 h and a fast increase until 17 h. Maximal uptake was achieved for ^{99m}Tc-Me/Pz(DTX)BCMs in the MDA-MB-231 and MNNG HOS cells (~12%). However, for the osteosarcoma cells the uptake profile of both type of micelles was similar. The lower cellular uptake was observed in the PC3 cell line. For this particular cell line the DTX entrapment did not improve the cellular uptake. Since the cell uptake is also dependent on particle size (Li et al., 2016; Varela et al., 2012) the observed profile can be attributed to the size distribution of the micelles. Our results show that besides the physicochemical properties, the uptake is also dependent on incubation time and the cell type (Varela et al., 2012). The lowest cellular uptake observed in the PC3 cell line is in agreement with the results obtained in the anti-proliferative activity studies (see above).

3.9. Biodistribution studies

Entrapment of a chemotherapeutic agent such as DTX in BCMs may enhance the blood circulation time and increase the DTX accumulation in the tumor by the EPR effect. Hence, preliminary biodistribution studies of the radiolabeled micelles (^{99m}Tc-Me/Pz(DTX)BCMs) were carried out in healthy BALB/c mice to evaluate their biodistribution profile. The biodistribution of the radiolabeled copolymer (^{99m}Tc-Pz-PEG-*b*-PCL) was also studied to get insight on the *in vivo* stability of the micelles. Data from these studies are shown in Figs. 8 and 9, respectively.

The radiolabeled micelles featured a long blood circulation time (24.5 ± 3.0 and 8.0 ± 2.0% I.A./g blood at 4 h and 24 h p.i., respectively). Relevant hepatic uptake was also found at 4 h p.i. (23.0 ± 3.0% I.A./g) that decreased at 24 h p.i. (12.8 ± 1.2% I.A./g) indicating the hepatobiliar path as the main elimination route. No high spleen uptake was found (<6.3 ± 1.7% I.A./g). The moderate hepatic and splenic uptakes cannot be assigned only to the micelle's size (approximately 59 nm) since Hoang et al., using similar micelles (approximately 58 nm, same amphiphilic copolymer and similar zeta-potential) obtained higher splenic uptake at 48 h p.i. (21 ± 6% I.A./g) (Hoang et al., 2009). Radioactivity accumulation detected in highly irrigated organs such as lungs and heart was believed to be nonspecific. Indeed, the slow washout from these organs that clear over time may be attributed to the high activity in the blood pool. In spite of the predominant hepatobiliar excretory pathway important kidney accumulation was also found (6.6 ± 0.7% I.A./g at 24 h p.i.) indicating the involvement of a renal elimination mechanism. The overall rate of radioactivity excretion was moderate (<50%) at 24 h p.i.).

The animal studies with the radiolabeled copolymer indicated that the overall biodistribution profile of ^{99m}Tc-Pz-PEG-*b*-PCL was quite different from that of the radiolabeled micelles, suggesting that these micelles did not dissociate *in vivo*. Indeed, the radioactivity remaining in the blood stream after administration

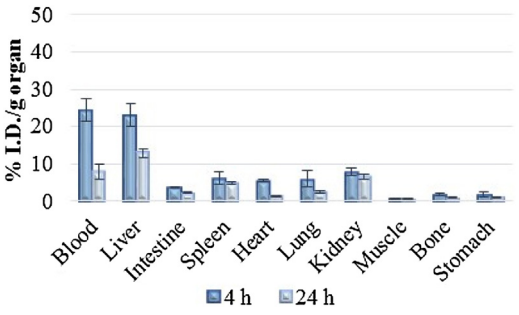

Fig. 8. Biodistribution of ^{99m}Tc- Me/Pz(DTX)BCMs micelles in BALB/c health mice at 4 h and 24 h p.i., expressed as%I.A./g.

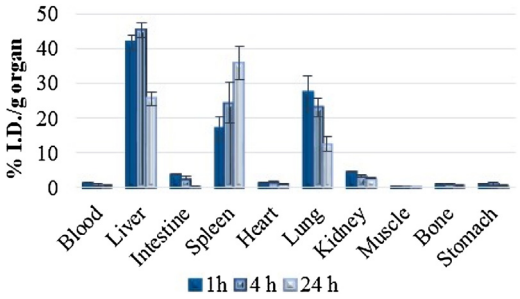

Fig. 9. Biodistribution of ^{99m}Tc- Pz-PEG-*b*-PCL copolymer in BALB/c health mice at 1 h, 4 h and 24 h p.i., expressed as%I.A./g.

of ^{99m}Tc-Pz-PEG-*b*-PCL was significantly lower (0.9 ± 0.3 and 0.6 ± 0.2% I.A./g blood at 4 h and 24 h p.i., respectively) than the radioactivity of the radiolabeled micelles (24.5 ± 3.0 and 8.0 ± 2.0% I.A./g blood at 4 h and 24 h p.i., respectively). On the contrary, the radioactivity accumulation in liver (45.3 ± 2.1 and 25.6 ± 1.9% I.A./g at 4 h and 24 h p.i., respectively) and spleen (24.4 ± 5.9 and 35.8 ± 4.8% I.A./g at 4 h and 24 h p.i., respectively) after injection of the radiolabeled copolymer was higher (2-fold and 7.5-fold at 24 h p.i., respectively) than in the case of the radiolabeled micelles (3.4 ± 0.4 and 2.7 ± 0.2% I.A./g at 4 h and 24 h p.i., respectively), while the kidney uptake (3.4 ± 0.4 and 2.7 ± 0.2 at 4 h and 24 h p.i., respectively) was much lower (0.4-fold) for the radiolabeled micelles (7.9 ± 1.0 and 6.6 ± 0.7 at 4 h and 24 h p.i., respectively). Moreover, the excretion of ^{99m}Tc-Pz-PEG-*b*-PCL was approximately 25% at 4 h p.i. whereas for the ^{99m}Tc-Me/Pz(DTX)BCMs was only 4.6%. However, the most striking difference observed was related to the pulmonary uptake, since an high accumulation of the radiolabeled copolymer was observed in lung (23.2 ± 2.7 and 12.5 ± 2.2% I.A./g at 4 h and 24 h p.i., respectively), compared to the radiolabeled micelles (6.0. ± 2.2 and 2.4 ± 0.4% I.A./g at 4 h and 24 h p.i., respectively), most likely due to the formation of aggregates with larger size than micelles.

In summary, the prolonged circulation lifetime in the bloodstream of the ^{99m}Tc-Me/Pz(DTX)BCMs, an essential feature, as well as its *in vivo* stability suggests their suitability as a drug delivery system into tumors by the EPR effect. This conclusion is in agreement with the studies of Lee, H. et al. that correlated the circulation half-life of different BCMs with their total intratumoral accumulation (Lee et al., 2010).

4. Conclusions

We have synthesized and characterized the new block copolymer Pz-PEG-*b*-PCL containing a pyrazolyl-diamine unit for stabilization of the organometallic core *fac*-$[M(CO)_3]^+$ (M = Re, Tc). This new copolymer was used to prepare functionalized non-loaded and DTX-loaded BCMs that were fully characterized. The resulting BCMs present a spherical morphology with hydrodynamic diameter (D_h) in the range of 30–70 nm. The *in vitro* DTX release study of loaded micelles has shown a pH-dependent behavior with a higher release at pH 5.0, when compared to physiological pH (7.4), a vital feature since the microenvironment in tumors are slightly acidic. Additionally, the DTX-loaded micelles present a higher anti-proliferative effect than DTX. Translated into an *in vivo* environment, these micelles should display a higher therapeutic efficacy against tumoral cells and lower side effects on normal tissues.

The functionalized micelles were radiolabeled with *fac*-$[^{99m}Tc(CO)_3]^+$ in high radiochemical yield and purity, affording ^{99m}Tc-BCMs, which are stable in PB pH 7.4 and in cell culture medium, at 37 °C. The cellular uptake studies with the radiolabeled micelles

are in agreement with the anti-proliferative studies, since higher accumulation in the cell lines result into a higher anti-proliferative activity. The biodistribution in healthy BALB/c showed a slow blood clearance and long half-life in the bloodstream, a required feature for the EPR effect.

These encouraging results prompt us to further explore these platforms in tumor animal models.

In conclusion, we have developed and evaluated DTX loaded micelles as prospective platforms for cancer therapy and, when radiolabeled with ^{99m}Tc, could be further explored for image-guided cancer theranostics.

Acknowledgments

This research was supported by the Fundação para a Ciência e Tecnologia (FCT) through the project EXCL/QEQ-MED/0233/2012 and carried out within European COST actions TD1004. C2TN/IST authors gratefully acknowledge the FCT support through the UID/Multi/04349/2013 project. Elisabete Ribeiro acknowledges the FCT research grant.

Appendix A. Supplementary data

Supplementary data associated with this article can be found, in the online version, at http://dx.doi.org/10.1016/j.ijpharm.2016.11.004.

References

Alberto, R., Ortner, K., Wheatley, N., Schibli, R., Schubiger, A.P., 2001. Synthesis and properties of boranocarbonate: a convenient in situ CO source for the aqueous preparation of (TC)-T-99m(OH2)(3)(CO)(3) (+). J. Am. Chem. Soc. 123 (13), 3135–3136.

Alexis, F., Pridgen, E., Molnar, L.K., Farokhzad, O.C., 2008. Factors affecting the clearance and biodistribution of polymeric nanoparticles. Mol. Pharm. 5 (4), 505–515.

Allen, C., Maysinger, D., Eisenberg, A., 1999. Nano-engineering block copolymer aggregates for drug delivery? Colloids Surf. B-Biointerfaces 16 (1–4), 3–27.

Alves, S., Paulo, A., Correia, J.D.G., Gano, L., Smith, C.J., Hoffman, T.J., Santos, I., 2005. Pyrazolyl derivatives as bifunctional chelators for labeling tumor-seeking peptides with the fac- M(CO)(3) (+) moiety (M = Tc-99m, Re): synthesis, characterization, and biological behavior. Bioconjug. Chem. 16 (2), 438–449.

Correia, J.D.G., Paulo, A., Raposinho, P.D., Santos, I., 2011. Radiometallated peptides for molecular imaging and targeted therapy. Dalton Trans. 40 (23), 6144–6167.

Diao, Y.-Y., Li, H.-Y., Fu, Y.-H., Han, M., Hu, Y.-L., Jiang, H.-L., Tsutsumi, Y., Wei, Q.-C., Chen, D.-W., Gao, J.-Q., 2011. Doxorubicin-loaded PEG-PCL copolymer micelles enhance cytotoxicity and intracellular accumulation of doxorubicin in adriamycin-resistant tumor cells. Int. J. Nanomed. 6, 1955–1962.

Ernsting, M.J., Murakami, M., Roy, A., Li, S.D., 2013. Factors controlling the pharmacokinetics, biodistribution and intratumoral penetration of nanoparticles. J. Control. Release 172 (3), 782–794.

Esmaeili, F., Dinarvand, R., Ghahremani, M.H., Amini, M., Rouhani, H., Sepehri, N., Ostad, S.N., Atyabi, F., 2009. Docetaxel-albumin conjugates: preparation, in vitro evaluation and biodistribution studies. J. Pharm. Sci. 98 (8), 2718–2730.

Estanqueiro, M., Amaral, M.H., Conceicao, J., Sousa Lobo, J.M., 2015. Nanotechnological carriers for cancer chemotherapy: the state of the art. Colloids Surf. B-Biointerfaces 126, 631–648.

Goncalves, C., Martins, J.A., Gama, F.M., 2007. Self-assembled nanoparticles of dextrin substituted with hexadecanethiol. Biomacromolecules 8 (2), 392–398.

Gothwal, A., Khan, I., Gupta, U., 2016. Polymeric micelles: recent advancements in the delivery of anticancer drugs. Pharm. Res. 33 (1), 18–39.

Guo, J.T., Hong, H., Chen, G.J., Shi, S.X., Zheng, Q.F., Zhang, Y., Theuer, C.P., Barnhart, T. E., Cai, W.B., Gong, S.Q., 2013. Image-guided and tumor-targeted drug delivery with radiolabeled unimolecular micelles. Biomaterials 34 (33), 8323–8332.

Hoang, B., Lee, H., Reilly, R.M., Allen, C., 2009. Noninvasive monitoring of the fate of In-111-labeled block copolymer micelles by high resolution and high sensitivity microSPECT/CT imaging. Mol. Pharm. 6 (2), 581–592.

Hoang, B., Reilly, R.M., Allen, C., 2012. Block copolymer micelles target auger electron radiotherapy to the nucleus of HER2-positive breast cancer cells. Biomacromolecules 13 (2), 455–465.

Kim, M.S., Hyun, H., Cho, Y.H., Seo, K.S., Jang, W.Y., Kim, S.K., Khang, G., Lee, H.B., 2005. Preparation of methoxy poly(ethyleneglycol)-block-poly(caprolactone) via activated monomer mechanism and examination of micellar characterization. Polym. Bull. 55 (3), 149–156.

Lee, H., Zeng, F.Q., Dunne, M., Allen, C., 2005. Methoxy poly(ethylene glycol)-block-poly(delta-valerolactone) copolymer micelles for formulation of hydrophobic drugs. Biomacromolecules 6 (6), 3119–3128.

Lee, H., Fonge, H., Hoang, B., Reilly, R.M., Allen, C., 2010. The effects of particle size and molecular targeting on the intratumoral and subcellular distribution of polymeric nanoparticles. Mol. Pharm. 7 (4), 1195–1208.

Li, S.D., Huang, L., 2008. Pharmacokinetics and biodistribution of nanoparticles. Mol. Pharm. 5 (4), 496–504.

Li, J., Wu, N., Wu, J., Wan, Y., Liu, C., 2016. Effect of protein adsorption on cell uptake and blood clearance of methoxy poly(ethylene glycol)-poly(caprolactone) nanoparticles. J. Appl. Polym. Sci. 133 (3) .

Liu, J., Zeng, F., Allen, C., 2007. In vivo fate of unimers and micelles of a poly(ethylene glycol)-block-poly(caprolactone) copolymer in mice following intravenous administration. Eur. J. Pharm. Biopharm. 65 (3), 309–319.

Liu, Z.H., Liu, D.H., Wang, L.L., Zhang, J.A., Zhang, N., 2011. Docetaxel-loaded pluronic P123 polymeric micelles: in vitro and in vivo evaluation. Int. J. Mol. Sci. 12 (3), 1684–1696.

Liu, J., Huang, Y.R., Kumar, A., Tan, A., Jin, S.B., Mozhi, A., Liang, X.J., 2014. pH-Sensitive nano-systems for drug delivery in cancer therapy. Biotechnol. Adv. 32 (4), 693–710.

Lou, X.D., Detrembleur, C., Jerome, R., 2002. Living cationic polymerization of delta-valerolactone and synthesis of high molecular weight homopolymer and asymmetric telechelic and block copolymer. Macromolecules 35 (4), 1190–1195.

Lu, Y., Park, K., 2013. Polymeric micelles and alternative nanonized delivery vehicles for poorly soluble drugs. Int. J. Pharm. 453 (1), 198–214.

Manchun, S., Dass, C.R., Sriamornsak, P., 2012. Targeted therapy for cancer using pH-responsive nanocarrier systems? Life Sci. 90 (11–12), 381–387.

Mikhail, A.S., Allen, C., 2009. Block copolymer micelles for delivery of cancer therapy: transport at the whole body, tissue and cellular levels. J. Control. Release 138 (3), 214–223.

Mikhail, A.S., Allen, C., 2010. Poly(ethylene glycol)-b-poly(epsilon-caprolactone) micelles containing chemically conjugated and physically entrapped docetaxel: synthesis, characterization, and the influence of the drug on micelle morphology. Biomacromolecules 11 (5), 1273–1280.

Mikhail, A.S., Eetezadi, S., Allen, C., 2013. Multicellular tumor spheroids for evaluation of cytotoxicity and tumor growth inhibitory effects of nanomedicines in vitro: a comparison of docetaxel-loaded block copolymer micelles and taxotere (R). Plos One 8 (4) .

Mikhail, A.S., Eetezadi, S., Ekdawi, S.N., Stewart, J., Allen, C., 2014. Image-based analysis of the size- and time-dependent penetration of polymeric micelles in multicellular tumor spheroids and tumor xenografts? Int. J. Pharm. 464 (1–2), 168–177.

Morais, M., Subramanian, S., Pandey, U., Samuel, G., Venkatesh, M., Martins, M., Pereira, S., Correia, J.D.G., Santos, I., 2011. Mannosylated dextran derivatives labeled with fac- M(CO)(3) (+) (M = Tc-99m, Re) for specific targeting of sentinel lymph node. Mol. Pharm. 8 (2), 609–620.

Muthu, M.S., Kutty, R.V., Luo, Z., Xie, J., Feng, S.-S., 2015. Theranostic vitamin E TPGS micelles of transferrin conjugation for targeted co-delivery of docetaxel and ultra bright gold nanoclusters. Biomaterials 39, 234–248.

Palma, G., Conte, C., Barbieri, A., Bimonte, S., Luciano, A., Rea, D., Ungaro, F., Tirino, P., Quaglia, F., Arra, C., 2014. Antitumor activity of PEGylated biodegradable nanoparticles for sustained release of docetaxel in triple-negative breast cancer? Int. J. Pharm. 473 (1–2), 55–63.

Perez-Herrero, E., Fernandez-Medarde, A., 2015. Advanced targeted therapies in cancer: drug nanocarriers, the future of chemotherapy. Eur. J. Pharm. Biopharm. 93, 52–79.

Raposinho, P.D., Correia, J.D.G., Oliveira, M.C., Santos, I., 2010. Melanocortin-1 receptor-targeting with radiolabeled cyclic alpha-melanocyte-stimulating hormone analogs for melanoma imaging. Biopolymers 94 (6), 820–829.

Ronquist, K.G., Sanchez, C., Dubois, L., Chioureas, D., Fonseca, P., Larsson, A., Ullen, A., Yachnin, J., Ronquist, G., Panaretakis, T., 2016. Energy-requiring uptake of prostasomes and PC3 cell-derived exosomes into non-malignant and malignant cells. J. Extracell. Vesicles 5.

Topel, O., Cakir, B.A., Budama, L., Hoda, N., 2013. Determination of critical micelle concentration of polybutadiene-block-poly(ethyleneoxide) diblock copolymer by fluorescence spectroscopy and dynamic light scattering. J. Mol. Liq. 177, 40–43.

Torchilin, V.P., 2007. Micellar nanocarriers: pharmaceutical perspectives. Pharm. Res. 24 (1), 1–16.

Varela, J.A., Bexiga, M.G., Aberg, C., Simpson, J.C., Dawson, K.A., 2012. Quantifying size-dependent interactions between fluorescently labeled polystyrene nanoparticles and mammalian cells. J. Nanobiotechnol. 10.

Vaz, C.V., Alves, M.G., Marques, R., Moreira, P.I., Oliveira, P.F., Maia, C.J., Socorro, S., 2012. Androgen-responsive and nonresponsive prostate cancer cells present a distinct glycolytic metabolism profile. Int. J. Biochem. Cell Biol. 44 (11), 2077–2084.

Wicki, A., Witzigmann, D., Balasubramanian, V., Huwyler, J., 2015. Nanomedicine in cancer therapy: challenges, opportunities, and clinical applications. J. Control. Release 200, 138–157.

Yang, X.Q., Deng, W.J., Fu, L.W., Blanco, E., Gao, J.M., Quan, D.P., Shuai, X.T., 2008. Folate-functionalized polymeric micelles for tumor targeted delivery of a potent multidrug-resistance modulator FG020326. J. Biomed. Mater. Res. Part A 86A (1), 48–60.

Zeng, F.Q., Lee, H., Allen, C., 2006. Epidermal growth factor-conjugated poly (ethylene glycol)-block-poly(delta-valerolactone) copolymer micelles for targeted delivery of chemotherapeutics. Bioconjug. Chem. 17 (2), 399–409.

Zhang, X.C., Jackson, J.K., Burt, H.M., 1996. Determination of surfactant critical micelle concentration by a novel fluorescence depolarization technique? J. Biochem. Biophys. Methods 31 (3–4), 145–150.